# International Journal of Engineering in Computer Science



E-ISSN: 2663-3590 P-ISSN: 2663-3582 Impact Factor (RJIF): 5.52 www.computersciencejournals.com/ijecs

IJECS 2025; 7(2): 57-66 Received: 14-06-2025 Accepted: 19-07-2025

# Amjed A Al-Mudhafar

Department of Avionics Technologies Engineering, Engineering Technical College, Al-Furat Al-Awsat Technical University, Iraq Design and fabrication reflectionless and Semireflectionless microwave diplexer

# Amjed A Al-Mudhafar

**DOI:** https://www.doi.org/10.33545/26633582.2025.v7.i2a.202

#### Abstract

This paper presents a new realization of reflectionless and semi-reflectionless diplexer design aimed at signal reflections suppression as well as enhancement the performance of RF front-end systems. Design a traditional diplexer with two second-order BPFs (band-pass filter), which are resonant at different frequencies. This base design was compact and efficient, using half-wavelength structure realized by inward-coupled open-loop resonators as the BPFs.

An Absorptive Stub was added to improve impedance matching of the diplexer and bottom plateinkle loss at the input port. At the junction of the two filters, we connected a stub with Step Impedance Resonator (SIR) structure loaded with a resistor (R1), called Filter3. It served, as its name implies, to take up those direct signals that would otherwise reflect back to the source and make the diplexer work fully reflectionless. The prototype was printed using a low-cost FR4 dielectric material with an er value of 4.6 and the thickness of the substrate was set as 1.5 mm. The size of the fabricated prototype was about 50.1 mm × 41.2 mm with SMA connectors connected to all ports. Excellent agreement with simulated results was observed in the case of measurements performed using an N9917A network analyzer. In more detail, over a frequency interval from 1.45 GHz to 2.8 GHz, the input matching bandwidth of the diplexer was wideband (S11 < 0 dB) with insertion losses of -5dB and -6dB at frequencies centered at 1.72GHz and 2.0 GHz respectively. Moreover, an equivalent qusi-reflectionless modified semi-a period of reflection for the absorptive stub is replaced by band stop filter-shaped resonator (BSF) loaded with resistor R2. This version achieved some reflection suppression but still could not reach the full broadband reflectionless performance of the original design. The results encourage the benefit of providing absorptive structures in order to realize efficient and reflectionless diplexers for contemporary RF applications.

Keywords: Microstrip, diplexer, resonator, qusi-reflectionless, semi-reflectionless, reflectionless

## Introduction

Background Wireless communication systems continue to evolve and the development of millimeter wave band systems are required due to high frequency range. For transmit receive isolation, duplexers (with two filters on different frequency ranges) are an example of such a component. Nevertheless, minimizing the reflection influence (which impairs the efficiency of signal transmission and stability of systems) is a key issue.

Hence, the opposite ends present non-reflective duplexers as the convenient solution. These elements prevent back reflection and greatly reduce signal loss. The non-reflective aspect allows signals to travel along the respective paths as intended, where the reflection would lead into signal distortion or interference and degrade system robustness and increase noise levels in the circuit. This design also leads to higher energy savings and lower losses which extends performance of a whole system [1].

The absence of a reflective shed allows these components to be integrated and used in portable or thin devices while maintaining performance. This design results in a better channel to channel isolation reducing interferance and hence improving the signal quality. This allows the majority of these devices to operate simultaneously in such multi-frequency environments without interference from reflections, which is preferable for a reliable operation and stable performance of the entire system <sup>[2]</sup>.

In [3] presents the design of an input-reflectionless low-pass filter (LPF) based on a multilayer diplexer architecture, which suppresses reflection and enhances stopband rejection through resistive loading and cascading.

Corresponding Author: Amjed A Al-Mudhafar Department of Avionics Technologies Engineering, Engineering Technical College, Al-Furat Al-Awsat Technical University, Iraq A two-layer microstrip prototype validated in measurement shows wide stopband and reflectionless behavior with performances that agree well with the simulation predictions. The multilayer structure, however, raises cost and design complexity issues that might constrain its usage in low-cost or small-scale systems. Presents a tunable reflectionless diplexer for the L-band using microstrip transmission lines, capable of both separating and combining frequencies with low insertion loss and frequency adjustability via varactor diodes. The design is supported by theoretical analysis using coupling matrices and even/odd mode techniques, with simulations carried out in ADS software. However, the reliance on varactor diodes may introduce nonlinearity and increase sensitivity to bias variations, affecting overall stability and performance in [4]. Introduces in [5-7] a high-order bandpass filtering dispersivedelay structure (DDS) with quasi-reflectionless behavior, using a complementary diplexer design where a resistively loaded auxiliary channel absorbs unwanted out-of-band signals. The design preserves the desired group-delay response and is realized through a two-step synthesis and optimization method, validated by a 2 GHz microstrip prototype. However, the complexity of the coupling-matrix synthesis and the need for precise component tuning can increase design time and limit scalability for broader applications. Presents in [8-10] a theoretically grounded method for designing matching networks that equalize gain while ensuring a constant input impedance, using two synthesized conductance functions in parallel. It offers improved size and efficiency compared to traditional balanced amplifier networks, making it especially suitable for MMIC implementations. However, practical limitations may arise from the precision required in synthesizing conductance functions, which could complicate fabrication and integration in high-frequency designs. Introduces in [11-<sup>13]</sup> an RF dispersive-delay structure (DDS) with quasireflectionless input, achieved by combining a main bandpass channel and a resistively loaded complementary bandstop channel. The design enables simultaneous DDS, BPF, and low-reflection functionality, with phase compensation ensuring the desired transmission profile. However, the added complexity of integrating and tuning dual-channel structures may increase design difficulty and sensitivity to fabrication tolerances. Proposes a planar in [14-<sup>16]</sup> wideband balanced-to-balanced microstrip diplexer that addresses signal reflection issues by incorporating frequency-specific reflectionless stubs at differential ports. The design is validated through a fabricated prototype showing broad bandwidth performance at 1.2 GHz and 1.8 GHz. However, the use of multiple stubs adds layout complexity and may complicate precise frequency alignment during fabrication. Introduces a compact diplexer design in [17] optimized for mid-band 5G systems, utilizing dual-band filters with coupled lines and novel resonators to cover four target frequencies. Theoretical analysis through even/odd mode and LC modeling supports accurate parameter extraction, while the prototype achieves low insertion loss and high efficiency in a small footprint. However, the close spacing of operating bands and intricate structure may pose challenges for isolation and fabrication precision in practical deployments. Presents a frequencyreconfigurable reflectionless micro strip bandpass filter in [18, 19] using a complementary-duplexer design, where the bandpass channel handles signal transmission and a

resistively terminated bandstop channel absorbs reflected energy. A two-stage tunable prototype operating from 0.8 to 1.1 GHz demonstrates the concept. However, the inclusion of tunable elements and dual-channel architecture increases design complexity and may introduce tuning instability or higher insertion loss. Introduces two high-selectivity inputreflectionless bandpass filter (BPF) in [20, 21] designs narrowband and wideband using a complementary-duplexer architecture that combines advanced resonator and transversal filtering techniques. Out-of-band signal energy is absorbed by a resistively loaded auxiliary channel, enabling reflectionless performance across the entire structure. However, the complexity of dual-path structures and precise alignment of transmission zeros may challenge practical fabrication and tuning accuracy. Presents a compact single/multi-band coupled-multiline filtering section based on N+1 quarter-wavelength transmission-line segments, enabling the creation of RF filters with multiple transmission zeros for enhanced selectivity [22, 23]. Several microstrip prototypes such as a dual-band diplexer, tripleband filters, and a filtering coupler-demonstrate the versatility of the design. However, as the number of bands increases, maintaining precise control over the coupling and transmission zero placement can become challenging, potentially affecting performance consistency across wide frequency ranges. Advances the concept of reflectionless filters [24, 25] by introducing new structures that enhance stopband attenuation and cutoff sharpness without compromising passband performance or reflectionless behavior. A key innovation is the use of a two-port subnetwork coupling the stopband terminations, along with designs where most reactive elements share equal normalized values, simplifying tuning and supporting integration. However, while equal-valued components ease implementation, the added sub-network may introduce design complexity and sensitivity to parasitic effects in high-frequency environments.

This approach is now improved upon by using cutting edge technology to reduce the reverse interference making reflectionless diplexers. It is this feature that is needed to increase the overall performance, decrease signal loss, and thus it will directly reflect efficiency and reliability in a wide range of applications from mobile phones to complex wireless system solutions. A duoband with the NRD mode can be very useful for a replication in future high-precision and efficient tech that will arise, such as the recently invented 5G communication systems or future wireless networks. Given the rapid advances in communication and computing, reflectionless duplexers clearly make a great deal of sense

Design of the duplexer was made in such way as to enable it for future upgrades, or customization in line with current app needs. This architecture enables the device to be highly configurable, thereby addressing the ever-changing and adapting needs of systems making it well-suited for next-generation wireless systems. A strict series of tests were completed on the prototypes to meet top technical requirements here, as illustrated in Figure 1, guaranteeing high performance.

To this end, we have designed and simulated the device under investigation by means of Advanced Design System (ADS) one of the most powerful engineering tools in the field of RF & microwaves design. Baked in to the program is capability around conveyor line technology to build

micro-strip components and analyse them, helping ensure they are able to deliver tight variability results for high quality manufacturing.

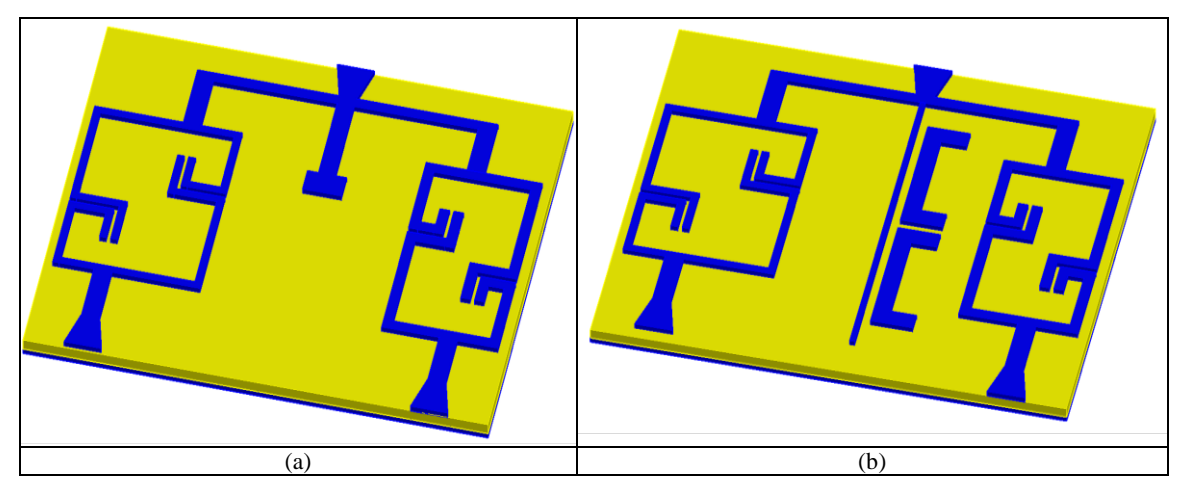


Fig 1: Proposed Diplexer (a) Reflectionless S11, (b) Semireflectionless S11

# Design reflectionless diplexer and fabrication

The circuit elements used in classic duplexers are not entirely matched, if they were they would all work but inevitably some frequencies will reflect a fraction of the signal transmitted and thus much energy being lost whilst interfering more. This has a drastic impact on signal quality, especially in systems that require precision performance such as Mobile phone; wireless communication equipment etc. On the contrary, an anechoic duplexer design prevents these reflections from occurring so that all input and output signals will truly meet the required specifications.

The Reflection-less duplexer is not just the next thing in duplexers, it is a re-imagining of how traditional duplexers can be improved. This kind of duplexer is efficient in signal processing and can minimize internal reflections detrimental for the quality of a signal. With advanced technology at its core, the design reduces reflection on the signal transmission during channel switching and significantly improves system stability as well as minimizes power losses

Initially, we designed a diplexer structure composed of two bandpass filters (BPFs), each operating at a different center frequency. Both filters are implemented using second-order open-loop resonators that are shaped as half-wavelength structures. Each resonator is inwardly folded to achieve compact size and improve integration illustrated in Figure 3. The detailed layout and dimensions of the resonators are illustrated in table 1. After verifying the basic performance of the diplexer, we enhanced the design by adding an absorptive stub. This stub is realized using a step impedance resonator (SIR) combined with a resistor. The addition of this component allows the diplexer to achieve reflectionless behavior across the operating bands. This improves both isolation and return loss, making the device more efficient for practical RF applications.

By <sup>[26]</sup> analysing the circuit topology of Figure 2, the equations of the input impedance for an absorptive stub can be derived from Eq.(1-2) when the resistance load value is  $R_L = 79.37$  ohms

$$Z_{X} = \frac{Z_{4}(R_{L} + jZ_{4} \tan \theta_{4})}{Z_{4} + jR_{L} \tan \theta_{4}}$$
 (1)

$$Z_{in-absorptive} = \frac{Z_{5}(Z_{4}(R_{L}+jZ_{4}\tan\theta_{4})+jZ_{5}(Z_{4}+jR_{L}\tan\theta_{4})\tan\theta_{5})}{Z_{5}(Z_{4}+jR_{L}\tan\theta_{4})+jZ_{4}(R_{L}+jZ_{4}\tan\theta_{4})\tan\theta_{2}} \tag{2}$$

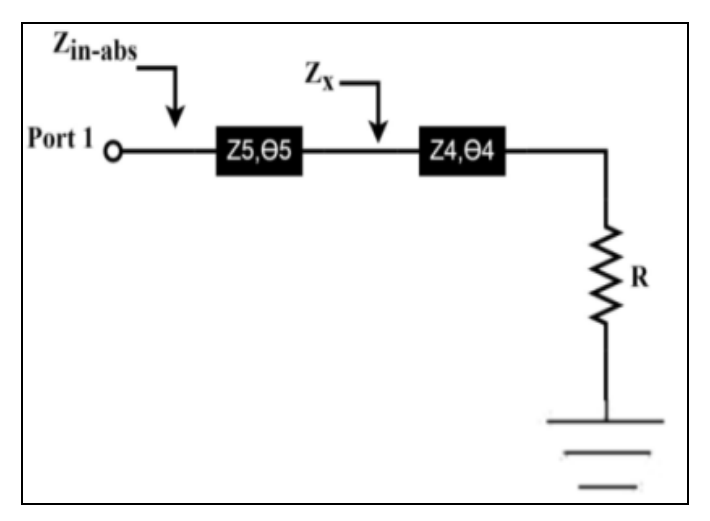


Fig 2: Layout absorptive band pass filter

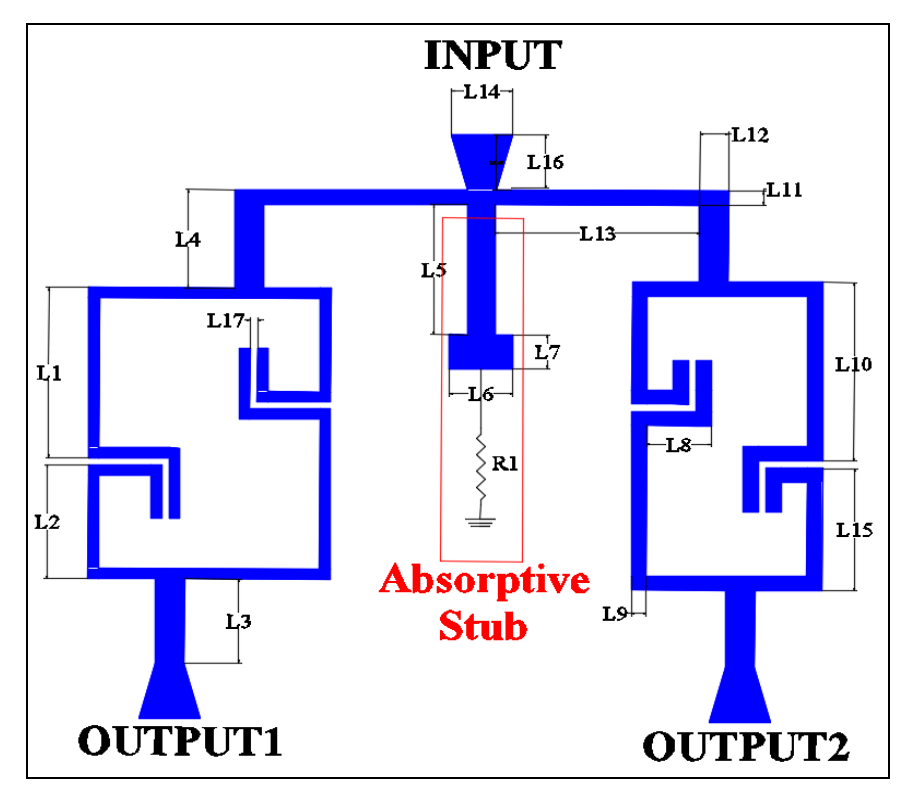


Fig 3: Microstrip reflectionless diplexer layout

The reflectionless diplexer was fabricated using a printed circuit board (PCB) made from FR4 substrate, which is commonly used in RF applications due to its low cost and acceptable electrical performance. The FR4 material has a dielectric constant (ɛr) of 4.6, a thickness of 1.5 mm, and a loss tangent of 0.01, which are suitable for prototyping microwave circuits. The conductive layer used for the layout was copper, with a standard thickness of 0.035 mm. Based on the previously discussed layout, which combines two

second-order bandpass filters using half-wavelength openloop resonators, the diplexer was realized with a compact footprint of 50.95 mm in width and 41.2 mm in length. An absorptive stub, implemented using a step-impedance resonator (SIR) loaded with a resistor, was integrated into the design to achieve reflectionless behavior. This addition ensures minimal return loss across both passbands, enhancing the isolation and power transfer.

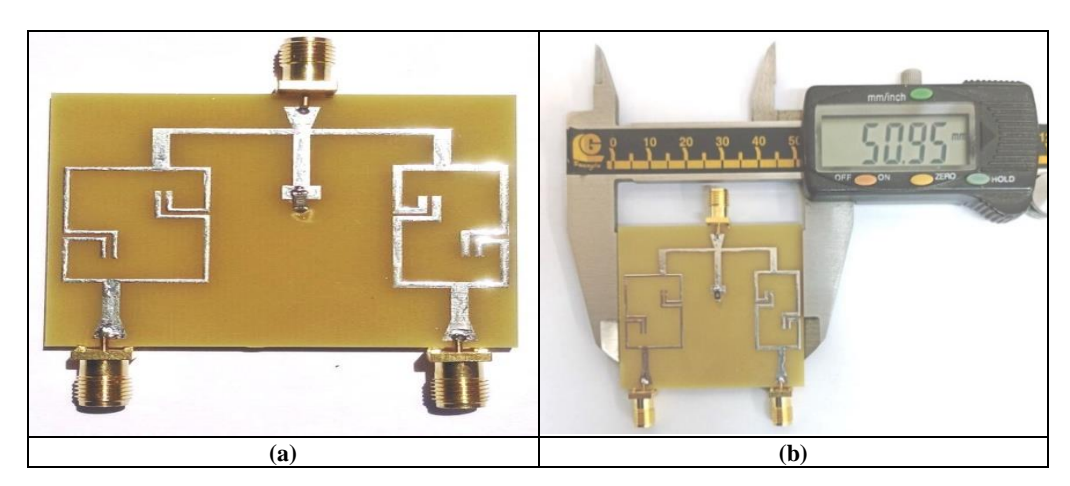


Fig 4: Photograph of fabricated microstrip reflectionless diplexer

To facilitate experimental validation, SMA connectors were mounted on the three ports of the diplexer, as clearly shown in Figure 3. The prototype was then prepared for full-wave simulation and measurement to compare the performance with the predicted results.

# **Simulation Results and Measurement**

This RF/microwave device uses an optional duplex architecture. It consists of a bandpass channel and a resistive end channel. The bandwidth determines the overall

transmission profile of the filter. The energy of the input signal not transmitted through this channel is absorbed by the input absorption-loaded buffer, as shown in Figure 5. This ensures that there are no reflections on the input of the filter. A theoretical basis for a dual filter without input reflections has been developed. We will receive a reflectionless response on both sides of our passband. We call it a reflectionless diplexer that operates at 1.72 GHz and 2GHz.

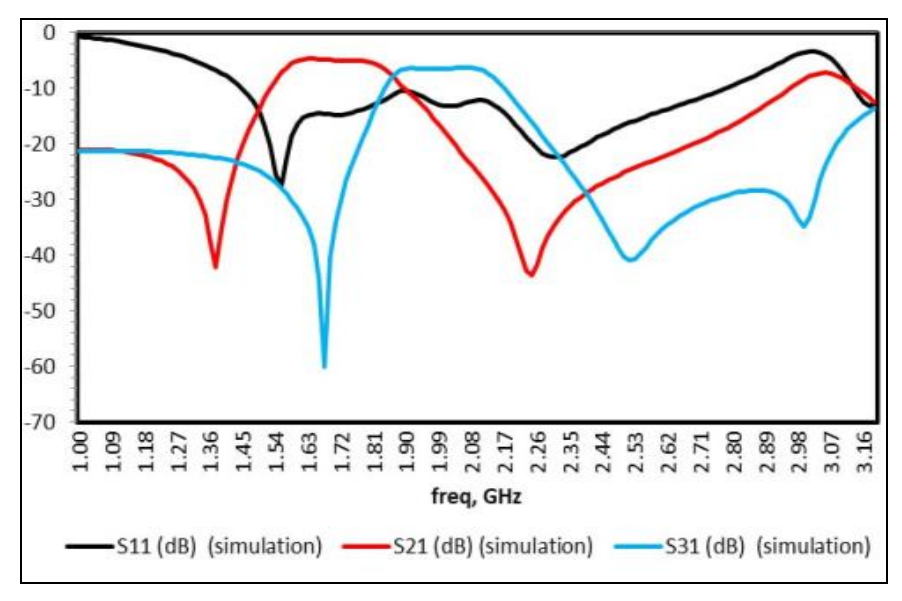


Fig 5: Simulated results of the proposed diplexer (S11), (S21) and (S31)

The measurement and characterization of the reflectionless diplexer were carried out using an N9917A Network Analyzer, as illustrated in Figure 6. The measurement results showed a strong correlation with the simulated data, confirming the effectiveness of the proposed design. The diplexer successfully operated at two distinct frequencies, corresponding to S21 and S31 transmission paths, centered at 1.72 GHz and 2.0 GHz, respectively. The insertion losses recorded were approximately -5 dB and -6 dB in each passband, as presented in Figure 5.

Furthermore, the return loss (S11) exhibited a wide rejection bandwidth with values consistently below 0 dB, which verifies the reflectionless performance of the diplexer. Specifically, the S11 remained below 0 dB across the extended frequency range from 1.45 GHz to 2.8 GHz,

indicating minimal signal reflection across this band. This broadband reflectionless behavior, as depicted in Figure 5, confirms that the absorptive structure integrated into the diplexer design performs effectively over a wide frequency range.

The two measured transmission zeros occurred at 1.35 and, 2.26 GHz for the lower band, and three transmission zeroes 1.66, 2.47, and 3.03GHz, while the measured out-of-band lower suppression at 1 to 1.35 GHz and above was then 20dB. Most of the simulated features agree well with the measurements, except for the upper range above 2.28GHz. This difference was noticed because the mass measured by the induction coil was lower than expected illustrated in Figure 7.



Fig 6: Photograph of fabricated microstrip reflectionless diplexer with N9917A network analyzer

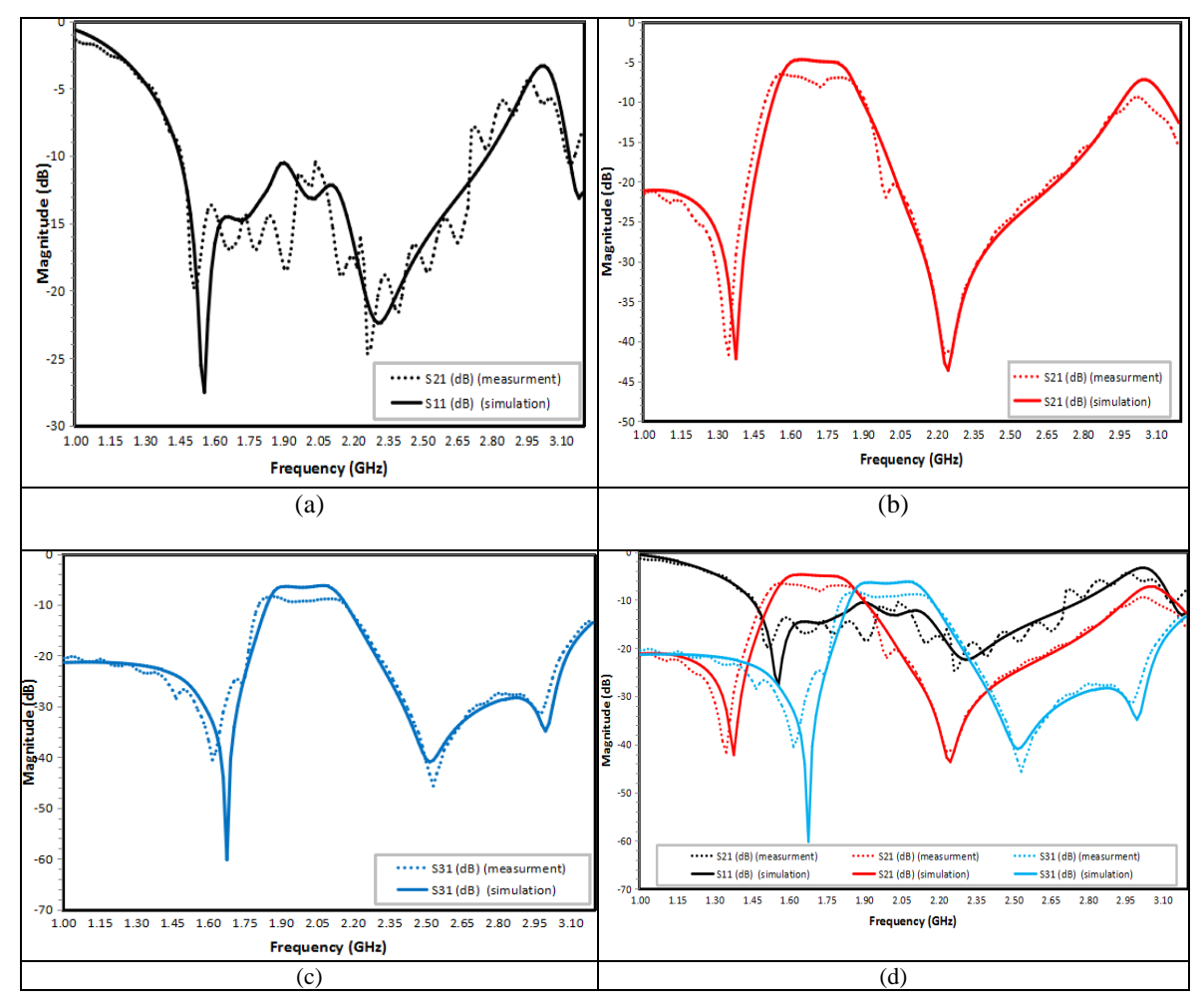


Fig 7: Measured and simulated results of the fabricated prototype reflectionless diplexer (a) S11, (b) S21 (c) S31, (d) all result

When comparing the same diplexer design with and without the presence of resistor R1, a significant difference in performance is observed, particularly in the return loss (S11) response. The removal of the resistor causes a noticeable degradation in return loss, with its value increasing sharply across the frequency band. This indicates a higher level of signal reflection back into the system, which negatively impacts the overall efficiency and

effectiveness of the diplexer. In contrast, when R1 is included in the design, the return loss remains considerably lower, reflecting better impedance matching and minimal signal reflection. As a result, the inclusion of R1 plays a critical role in enhancing the system's performance by reducing unwanted losses and improving the reflectionless characteristics of the device shown in Figure 8.

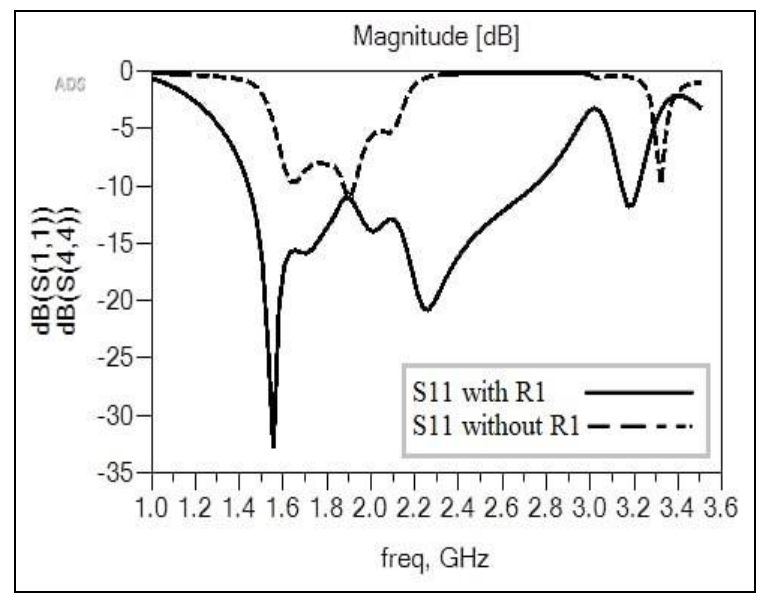


Fig 8: Compare the return losses between the result with and without R1

#### Design semi-reflectionless diplexer

To develop a Semi-Reflectionless Diplexer, we modified the previously designed structure by replacing the original absorptive stub with a new configuration. As shown in Figure 9, the absorptive element was redesigned as a Band-

Stop Filter (BSF) using a second-order half-wavelength resonator. This resonator is implemented in a C-shaped geometry to achieve compactness and effective coupling within the available substrate area.

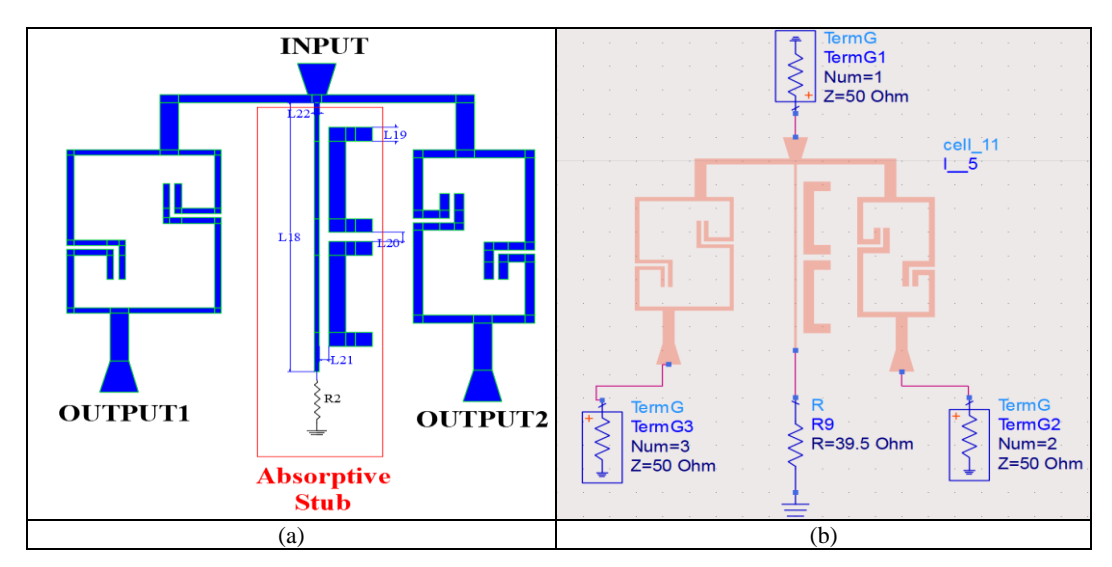


Fig 9: (a) semi-reflectionless diplexer layout, (b) schematic

The main difference in this new configuration is the directional reflectionless behavior. A resistor labeled as R2 is connected across the BSF, enabling it to absorb unwanted reflected signals from one side of the diplexer only. Unlike the full reflectionless diplexer, which ensures no signal reflection from either port, this semi-reflectionless structure is optimized for single-ended absorption. This means only one side of the diplexer (typically the source side) will exhibit minimal reflection (low S11), while the other side

may still reflect energy. This approach significantly reduces the complexity and cost of the design while still offering the key benefit of reduced signal degradation from reflection. The impact of this configuration is clearly illustrated in Figure 10, which shows the simulated performance metrics including insertion loss and return loss. The design remains based on the same substrate and dimensional footprint as the original diplexer, ensuring manufacturing compatibility and ease of integration into existing systems.

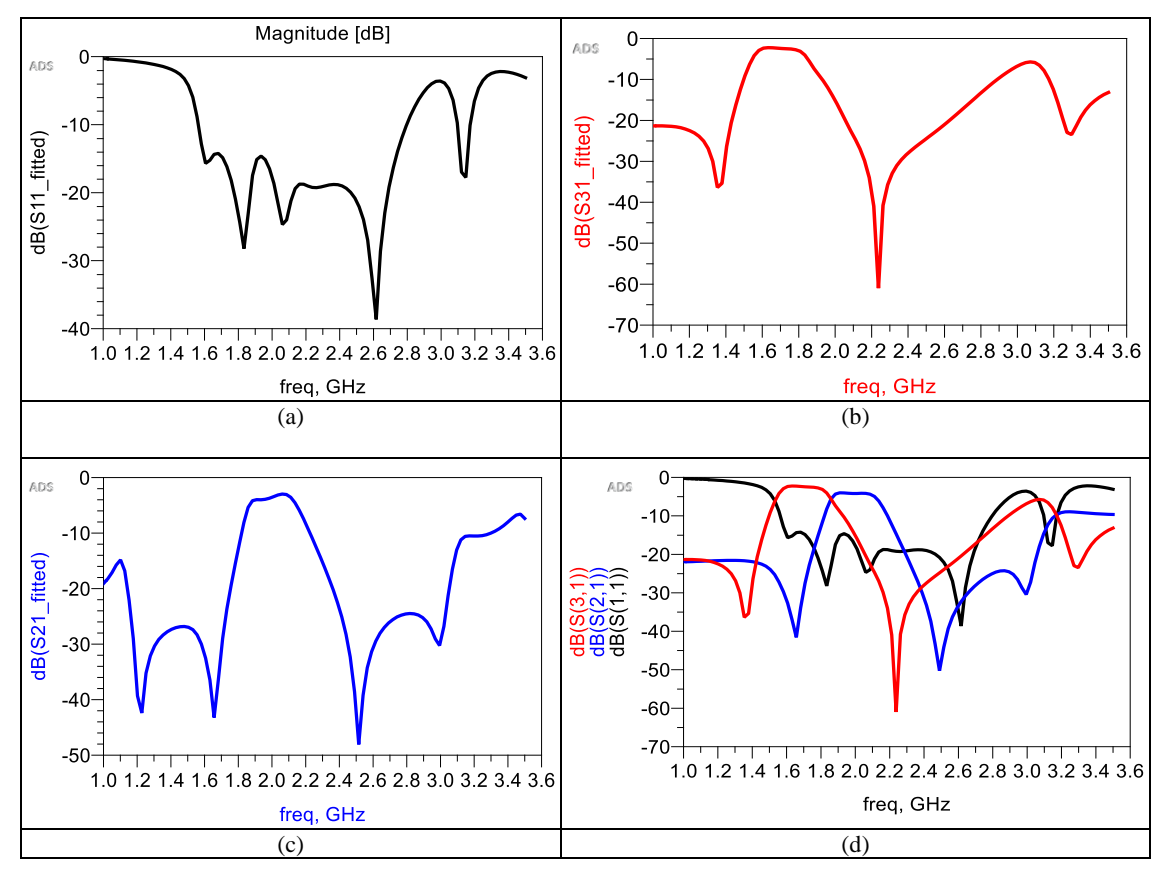


Fig 10: Simulated results of the fabricated prototype semi-reflectionless diplexer (a) S11 (b)S21 (c) S31 (d) all result

Figure 11 compares corresponding to simulation results a difference in the S11 as a function of frequency between the Reflectionless and the Semi-Reflectionless diplexers. As seen by the highly reflectionless measurement results, S11 (return loss) is maintained well below -10dB across a wide frequency range for the fully integrated design showing good impedance matching and minimal reflected power from both ports. This aids in the overall system stability and improved signal integrity as a result.

Meanwhile, the semi-reflectionless layout which absorbs reflections only from one side, reveals a deterioration in S11 performance at the non-absorbing port. While S11 is still well within the acceptable range for most applications, some bandwidth and depth is lost compared to the fully reflectionless case. Because of where the absorptive stubs are placed and the resistor integration choice, this trade-off is even stronger.

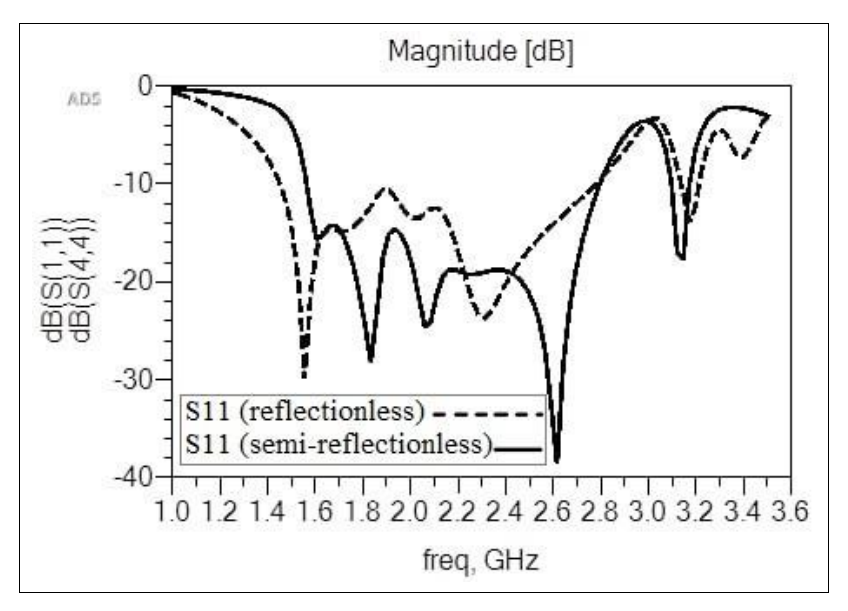


Fig 11: Compare the return losses between the reflectionless and semi-reflectionless diplexer

Parameters	Values
L1	12.03 mm
L2	8.03 mm
L3	5.94 mm
L4	6.94 mm
L5	9.2 mm
L6	4.2 mm
L7	2.39 mm
L8	4.24 mm
L9	0.99 mm
L10	12.62 mm
L11	1 mm
L12	1.9 mm
L13	13.51 mm
L14	4 mm
L15	8.62 mm
L16	3.91 mm
L17	2.93 mm
L18	33.78 mm
L19	1.72 mm
L20	1.13 mm
L21	1 mm
L22	0.5 mm
R1	100 ohm
R2	39.5 ohm

# Conclusion

This study reports the alternative configurations and investigates the design consideration, fabrication processes of both reflectionless and semi-reflectionless, where open-loop and step impedance resonator architectures based diplexer structures were developed. Initially, a standard diplexer was developed with two second-order bandpass filters with a pair of inductive coupled open-loop resonators

necessarily matched by the allowed bands. The structure was further modified to a Reflectionless Diplexer by incorporating an Absorptive Stub, realized through a Step Impedance Resonator (SIR) loaded with a resistor which helped in reducing the impeding effects of signal reflections; thereby improving system performance. FR4 was chosen as the substrate, keeping the overall size small and allowing for cheap fabrication, with SMA connectors in

all ports.

.Measurements were conducted using an N9917A Network Analyzer, and the results showed excellent agreement with simulations. The Reflectionless Diplexer achieved wideband matching characteristics with S11 consistently below 0 dB across the 1.45 GHz to 2.8 GHz range. Insertion losses were approximately -5 dB and -6 dB at 1.72 GHz and 2.0 GHz, respectively. In contrast, when the resistor in the Absorptive Stub (R<sub>1</sub>) was removed, a noticeable increase in return loss was observed, leading to degraded system performance.

Further development was carried out to design a semireflectionless diplexer by replacing the full absorptive stub with a band stop filter (BSF)-shaped resonator loaded with a resistor (R2). This modification enabled reflection suppression only on one signal path. While the semireflectionless structure showed partial improvement in S11, it did not match the wideband low-reflection performance of the fully reflectionless design.

Therefore, it is evident from both simulation and measurement results that integrating a properly designed absorptive stub is crucial for achieving a true reflectionless The Reflectionless Diplexer response. significantly enhances signal integrity and system efficiency, especially high-frequency RF applications. While reflectionless designs may offer layout flexibility, they compromise on full-band matching. Thus, the reflectionless configuration remains the optimal solution for applications demanding minimal reflection and high performance. Through the proposed design, we notice a significant difference in terms of the presence of reflections compared to other designs, which helps increase the signal strength and protect it from losses.

#### References

- Pozar DM. Microwave engineering. Fourth Editions, University of Massachusetts at Amherst, John Wiley & Sons, Inc; 2012, p. 26-30.
- Morgan MA. Reflectionless filters. Artech House; 2017 Jan 31.
- 3. Yang L, Gómez-García R, Muñoz-Ferreras JM, Zhang R. Input-reflectionless low-pass filter on multilayered diplexer-based topology. IEEE Microwave and Wireless Components Letters. 2020 Aug 28;30(10):945-948.
- 4. Taghvaei A, Bayderkhani R, Espahbodi M. design and fabrication of adjustable reflectionless microstrip diplexer for L-band. Progress In Electromagnetics Research C. 2022 Nov 15;126:173-181.
- Jasinski M, Lamecki A, García GR, Mrozowski M. RF-Input-quasi-reflectionless filtering dispersive-delay structures based on complementary-diplexer architectures. IEEE Transactions on Microwave Theory and Techniques; 2025 Feb 27.
- 6. Wu X, Li Y, Liu X. Quasi-reflectionless microstrip bandpass filters with improved passband flatness and out-of-band rejection. IEEE Access. 2020 Sep 2;8:160500-14.
- García GR, Ferreras MJM, Feng W, Psychogiou D. Balanced symmetrical quasi-reflectionless single-and dual-band bandpass planar filters. IEEE Microwave and Wireless Components Letters. 2018 Aug 3;28(9):798-800.
- 8. McKay TG. Reflectionless broad-band matching networks using a diplexer approach. In1992 IEEE

- MTT-S Microwave Symposium Digest, IEEE; 1992 Jun 1, p. 1477-1480.
- 9. Morgan MA, Groves WM, Boyd TA. Reflectionless filter topologies supporting arbitrary low-pass ladder prototypes. IEEE Transactions on Circuits and Systems I: Regular Papers. 2018 Oct 12;66(2):594-604.
- Zhao XB, Wei F, Yang L, García GR. Two-layer-magic-t-based bandpass, quasi-bandstop, and dual-passband balanced filters with differential-/common-mode reflectionless behavior. IEEE Transactions on Microwave Theory and Techniques. 2023 Sep 6:72(4):2267-2282.
- 11. Jasinski M, Lamecki A, Garcia GR, Mrozowski M. RF input-quasi-reflectionless dispersive-delay structures based on complementary-diplexer circuits. In2024 IEEE International Microwave Filter Workshop (IMFW), IEEE; 2024 Feb 21, p. 61-64.
- 12. Alkhuwaildi BH, Alkhafaji N. Third Order U-Shaped quasi-reflectionless bandpass filter. Progress in Electromagnetics Research C; 2022 Sep 1, p. 123.
- 13. Morgan MA. Think outside the band: Design and miniaturization of absorptive filters. IEEE Microwave Magazine. 2018 Oct 11;19(7):54-62.
- Zhao S, Wang Z, Gao M, Liu H, Fang S. Planar wideband balanced-to-balanced microstrip diplexer with reflectionless characteristics. AEU-International Journal of Electronics and Communications. 2024 Apr 1;177:155201.
- Fan M, Song K, Yang L, García GR. Balanced-circuitbased dual-band bandpass filter with symmetrical reflectionless behavior. In2021 IEEE Radio and Wireless Symposium (RWS), IEEE; 2021 Jan 17, p. 141-143.
- García GR, María FJM, Psychogiou D. Split-type inputreflectionless multiband filters. IEEE Microwave and Wireless Components Letters. 2018 Sep 18;28(11):981-3
- 17. Khani S, Roshani S, Roshani S, Fouladian M. Design and fabrication of an ultra small quadband diplexer integrated with a diplexed power amplifier for mid band 5G applications. Scientific Reports. 2025 Feb 11:15(1):5087.
- 18. Psychogiou D, García GR. Tunable reflectionless microstrip bandpass filters. In2018 IEEE Radio and Wireless Symposium (RWS), IEEE; 2018 Jan 15, p. 49-51.
- Bhavanam SN, Jalil Q. OFDM Channel Analysis Between FFT and Wavelet Transform Techniques. International Journal of Emerging Technologies in Computational and Applied Sciences; 2015 Feb, p. 2279-0055.
- 20. Feng W, Ma X, Shi Y, Shi S, Che W. High-selectivity narrow-and wide-band input-reflectionless bandpass filters with intercoupled dual-behavior resonators. IEEE Transactions on Plasma Science. 2020 Feb 4;48(2):446-54
- 21. Zhang Y, Wu Y, Wang W, Yan J. High-performance common-and differential-mode reflectionless balanced band-pass filter using coupled ring resonator. IEEE Transactions on Circuits and Systems II: Express Briefs. 2021 Aug 9;69(3):974-978.
- 22. Garcia GR, Yang L, Ferreras MJM, Psychogiou D. Single/multi-band coupled-multi-line filtering section and its application to RF diplexers, bandpass/bandstop

- filters, and filtering couplers. IEEE Transactions on Microwave Theory and Techniques. 2019 Aug 26;67(10):3959-72.
- 23. Yu W, Rao Y, Qian HJ, Luo X. Reflectionless filtering 90° coupler using stacked cross coupled-line and loaded cross-stub. IEEE Microwave and Wireless Components Letters. 2020 Apr 22;30(5):481-484.
- 24. Morgan MA, Boyd TA. Reflectionless filter structures. IEEE Transactions on Microwave Theory and Techniques. 2015 Feb 25;63(4):1263-1271.
- 25. García GR, Ferreras MJM, Psychogiou D. Adaptive multi-band negative-group-delay RF circuits with low reflection. IEEE Transactions on Circuits and Systems I: Regular Papers. 2021 Feb 8;68(5):2196-209.
- 26. Hong JS, Lancaster MJ. Microstrip filters for RF/microwave applications. John Wiley & Sons; 2004 Mar 24.